

A Holistic *In Silico* Approach to Find Novel Inhibitors for ErbB1 and ErbB2 Kinases

Jian-Bin Hu^{1*}, Ming-Jun Dong^{2,3#} and Jun Zhang^{3*}

¹Department of Radiation Oncology, Sir Run Run Shaw Hospital, Affiliated to Zhejiang Medical University, Hangzhou 310016, China

²Department of Anus and Intestine, Ningbo No.2 Hospital, Ningbo 315000, China

³Department of Cardiothoracic Surgery, the PLA 117 Hospital, Hangzhou 310013, China

*Authors contributed equally to this work

Abstract

Lung cancer is the primary cause of cancer deaths worldwide. The two major forms of lung cancer are non-small cell lung cancer and small cell lung cancer, which account for 85% and 15% of all lung cancers, respectively. There are around 26 genes which are involved in most of the lung cancers, among which ErbB1 and ErbB2 are the most prominent. Combined chemotherapy is used to cure cancer, which increases the side-effects, and the drugs available also show severe adverse reactions. Thus, there is a dire need for the search of novel inhibitors with fewer side-effects. Molecules obtained from natural sources have less side-effects. Therefore, the current study focuses on finding a common inhibitor from available natural products and FDA approved drugs, which bind with both ErbB1 and ErbB2. A variety of approaches have been adopted in this study, including sequence and structure analysis, 3D pharmacophore, docking studies, ADME prediction, and toxicity prediction. An *in silico* study confirmed the five phytochemicals Hyoscyamine, Cannabidiol, Cocinchinenone D, Cannabidiol E, and Heliotropamide and five FDA approved drugs Fesoterodine, Antrafenine, Fluspirilene, Posaconazole, and Iloprost to be potential inhibitors of both ErbB1 and ErbB2, which need to be confirmed through *in vivo* studies.

Keywords: Receptor tyrosine kinases; ErbB1; ErbB2; Natural products; Pharmacophore; Docking; ADME

Introduction

The incidence of lung cancer among cancer patients worldwide is 13%. The highest incidence is in developed countries, particularly in North America and Europe, and is less common in developing and underdeveloped countries [1-3]. Receptor tyrosine kinases (RTKs), which form a member of the epidermal growth factor receptor family, are involved in lung cancer proliferation. The four structurally related family members are ErbB1 (also known as EGFR or Her1), ErbB2 (also known as Her2 or Neu), ErbB3 (also known as Her3), and ErbB4 (also known as Her4). Among these, ErbB1 and ErbB2 are predominant in lung cancer [2,4,5]. All proteins have an extracellular ligand binding domain, a single hydrophobic transmembrane domain, and an intracellular tyrosine kinase domain. The success rate of antibody treatment targeting the extracellular ligand binding domain is low. The tyrosine kinase domain, which is structurally conserved in both ErbB1 and ErbB2, is the target site for most of the successful anti-cancer drugs which block its kinase activity. Many previous studies have adapted a dual targeting approach-inhibiting ErbB1 and ErbB2 concurrently-which provides synergistic inhibition [6,7]. The current study also follows the same approach, but the difference being that we focus on single inhibitor targeting both proteins, unlike the previous approaches which have considered individual inhibitors for each protein. This novel approach was successfully implemented to find a common inhibitor for the beta subunit of DNA polymerase III [8].

Materials and Methods

Protein primary sequence and structure retrieval

The primary sequences of ErbB1 (UniProt ID: P00533) and ErbB2 (UniProt ID: P04626) were retrieved from Universal Protein Resource (UniProt), which is a comprehensive resource for protein sequence and annotation data (www.uniprot.org). The three-dimensional structures of ErbB1 (PDB ID: 4G5J) and ErbB2 (PDB

ID: 3PP0) were obtained from Protein Data Bank (PDB) (www.rcsb.org), which is a single worldwide archive of structural data of biological macromolecules.

Sequence and structure analysis

Although ErbB1 has four isoforms produced by alternative splicing, only the first isoform is primarily involved in lung cancer (www.uniprot.org/uniprot/P00533) [9]. ErbB2 has five isoforms (www.uniprot.org/uniprot/P04626). To understand the similarities and dissimilarities of the kinase domain of these isoforms, sequence comparison was performed for each protein separately using the Clustal Omega program of UniProt (www.uniprot.org/align/). The three-dimensional structures of both the proteins were compared by jCE algorithm [10] of RCSB PDB Protein Comparison Tool (www.rcsb.org/pdb/workbench/workbench.do).

Ligand library construction

Natural products containing 6,160 compounds from marine sources and 18,151 compounds from medicinal plants were retrieved from previous extensive literature studies [11,12], Dr. Duke's Phytochemical library (www.ars-grin.gov/duke/), and PubChem BioAssay (www.ncbi.nlm.nih.gov/pcassay), which contains the bioactivity screens of chemical substances. Reference approved

*Corresponding author: Jun Zhang, Department of Cardiothoracic Surgery, the PLA 117 Hospital, No. 14 Lingyin Road, Hangzhou, Zhejiang 310013, China, Tel: 0086-571-87964033; Fax: 0086-571-87964033; E-mail: junzhang7070@gmail.com

Received December 15, 2015; Accepted March 01, 2016; Published March 08, 2016

Citation: Hu JB, Dong MJ, Zhang J (2016) A Holistic *In Silico* Approach to Find Novel Inhibitors for ErbB1 and ErbB2 Kinases. J Microb Biochem Technol 8: 151-160. doi: 10.4172/1948-5948.1000278

Copyright: © 2016 Hu JB, et al. This is an open-access article distributed under the terms of the Creative Commons Attribution License, which permits unrestricted use, distribution, and reproduction in any medium, provided the original author and source are credited.

drug molecules Afatinib (DrugBank ID: DB08916) and Lapatinib (DrugBank ID: DB01259), as well as the 1,543 molecules of FDA approved drugs were obtained from DrugBank (www.drugbank.ca). Since the approved drugs were selected because of their FDA approval, they did not require pre-clinical trials. DrugBank is a comprehensive, high-quality, freely accessible, online database containing information on drugs and drug targets. Both the drugs bind irreversibly with the kinase domain of the targets [6].

Ligand preparation and ADME prediction

The ligands used for the docking studies were prepared using LigPrep [13] of Maestro version 9.0 [14]. It is a robust collection of tools designed to prepare high quality, all-atom 3D structures for large numbers of drug-like molecules, starting with 2D or 3D structures in SD or Maestro format. Hydrogens were added to the ligands. The original state of the ligands was retained. The ligand was desalted and tautomers were generated. Specified chiralities of the ligand were maintained. Low energy ring conformation was generated from each ligand. The geometry was optimized using forcefield OPLS 2005. The output file was generated in the sdf file format.

QikProp was performed for the natural product molecules obtained from LigPrep. This application was used to determine the Absorption, Distribution, Metabolism, and Excretion (ADME) property [15]. Thirty one QikProp parameters were considered for each molecule. It is widely known that QikProp can efficiently evaluate pharmaceutically relevant properties for over half a million compounds in one hour, making it an indispensable lead generation and lead optimization tool. The molecules that passed ADME prediction were used for further procedures.

3D pharmacophore modelling and virtual screening

A pharmacophore is defined as a 3D structural feature that illustrates the interaction of a ligand molecule with a target receptor in a specific binding site [16]. It is possible to compute the shared pharmacophore feature of a known drug when its three-dimensional structure is available. To this end, virtual screening of the ligand based 3D pharmacophore was performed using LigandScout [17,18]. The reference drug molecules Afatinib (DrugBank ID: DB08916) and Lapatinib (DrugBank ID: DB01259) were optimized by LigPrep of Maestro version 9.0. Both the optimized structures were loaded onto the LigandScout, which were then aligned based on the pharmacophore features. Virtual screening was then performed with the generated shared feature against the natural products database and approved drug database created from the molecules obtained from the previous step which are passed from the *in silico* ADME prediction. The “pharmacophore-fit” scoring function, “match all query features” screening mode, and “get best matching conformation” retrieval mode were used for the pharmacophore search. The screened molecules were further confirmed by docking study.

Molecular docking

Molecular docking studies were carried out for both the proteins separately with both the datasets natural product and approved drugs using Molegro Virtual Docker (MVD). It has two docking search algorithms: MolDock Optimizer and MolDock Simplex Evolution (SE). MolDock Optimizer is the default search algorithm in MVD. In order to dock the receptor and ligand, the receptor was prepared from the “prepare molecule” option provided. Then, for grid searching, cavities were generated using the “detect cavity” option. Finally, the ligands obtained from the pharmacophore studies were provided in an sdf

704	LRILKETE	FKKIKVLGSGAFGTVYKGLWIPPEGEKVKIPVAIKELREATSPKANKEILDEA	763	P00533	EGFR_HUMAN
406	-----	-----	405	P00533-2	EGFR_HUMAN
683	-----	WGG--CSHLHAWPSASVIITASS-----	703	P00533-3	EGFR_HUMAN
629	-----	-----	628	P00533-4	EGFR_HUMAN
764	YVMASVDNPHVCRLLGICLTSTVQLITQLMPFGCLLDYVREHKDNIQSQYLLNWCVQIAK		823	P00533	EGFR_HUMAN
406	-----	-----	405	P00533-2	EGFR_HUMAN
704	-----	CH-----	705	P00533-3	EGFR_HUMAN
629	-----	-----	628	P00533-4	EGFR_HUMAN
824	GMNYLEDRRRLVHRDLAARNVLVKT PQHVKITDFGLAKLLGAEKEKYHAEGGKVP I KWMAL		883	P00533	EGFR_HUMAN
406	-----	-----	405	P00533-2	EGFR_HUMAN
706	-----	-----	705	P00533-3	EGFR_HUMAN
629	-----	-----	628	P00533-4	EGFR_HUMAN
884	ESILHRIYTHQSDVWSYGVTVWELMTFGSKPYDGIPASEISSILEKGERLPQPPICTIDV		943	P00533	EGFR_HUMAN
406	-----	-----	405	P00533-2	EGFR_HUMAN
706	-----	-----	705	P00533-3	EGFR_HUMAN
629	-----	-----	628	P00533-4	EGFR_HUMAN
944	YMIMVKCW MIDADSRPKFRELIIEFSK MARDPQRYLVIQGDERMHLPSPTDSNFYRALMD		1003	P00533	EGFR_HUMAN
406	-----	-----	405	P00533-2	EGFR_HUMAN
706	-----	-----	705	P00533-3	EGFR_HUMAN
629	-----	-----	628	P00533-4	EGFR_HUMAN

Figure 1: ERBB1- Kinase domain: sequence alignment of all 4 Isoform. Amino acid sequence of kinase domain is highlighted.

file format for docking using the docking wizard. During docking, the following parameters were fixed: number of runs 10, population size 50, crossover rate 0.9, scaling factor 0.5, maximum iteration 2,000, and grid resolution 0.30 [19]. Shared molecules capable of inhibiting both the proteins and which have better docking scores than the reference drug molecules were used for further study.

Toxicity prediction

Toxpredict (apps.ideaconsult.net:8080/ToxPredict) from the OpenTox server [20] was used to predict the toxicity of the natural product molecules obtained from the docking studies

Visualization of results

Molegro Virtual Docker (MVD) software, which is an integrated platform for predicting protein–ligand interactions, was used to visualize the docked result. This software handles all aspects of the docking process from preparation of the molecules to determination of the potential binding sites of the target protein, and prediction of the binding modes of the ligands [19].

Results and Discussion

Sequence and structure analysis

The retrieved isoform sequences of ErbB1 and ErbB2 were aligned independently. The kinase domain of isoform1 of ErbB1 did not show any significant similarities with that of the other three isoforms (Figure 1). Previous studies have demonstrated that only the first isoform is essentially involved in lung cancer (www.uniprot.org/uniprot/P00533) [9]. On the contrary, the kinase domains of all the five isoforms of ErbB2 show significant similarities (Figure 2).

The three-dimensional structures of both the proteins were compared by the jCE algorithm. The kinase domains of both the proteins showed higher similarity with RMSD: 1.68, identities: 73% and similarities: 83% (Figure 3), which indicates that a common inhibitor may be inhibiting both the proteins.

ADME prediction

It was determined from ADME prediction that from 24,311 natural

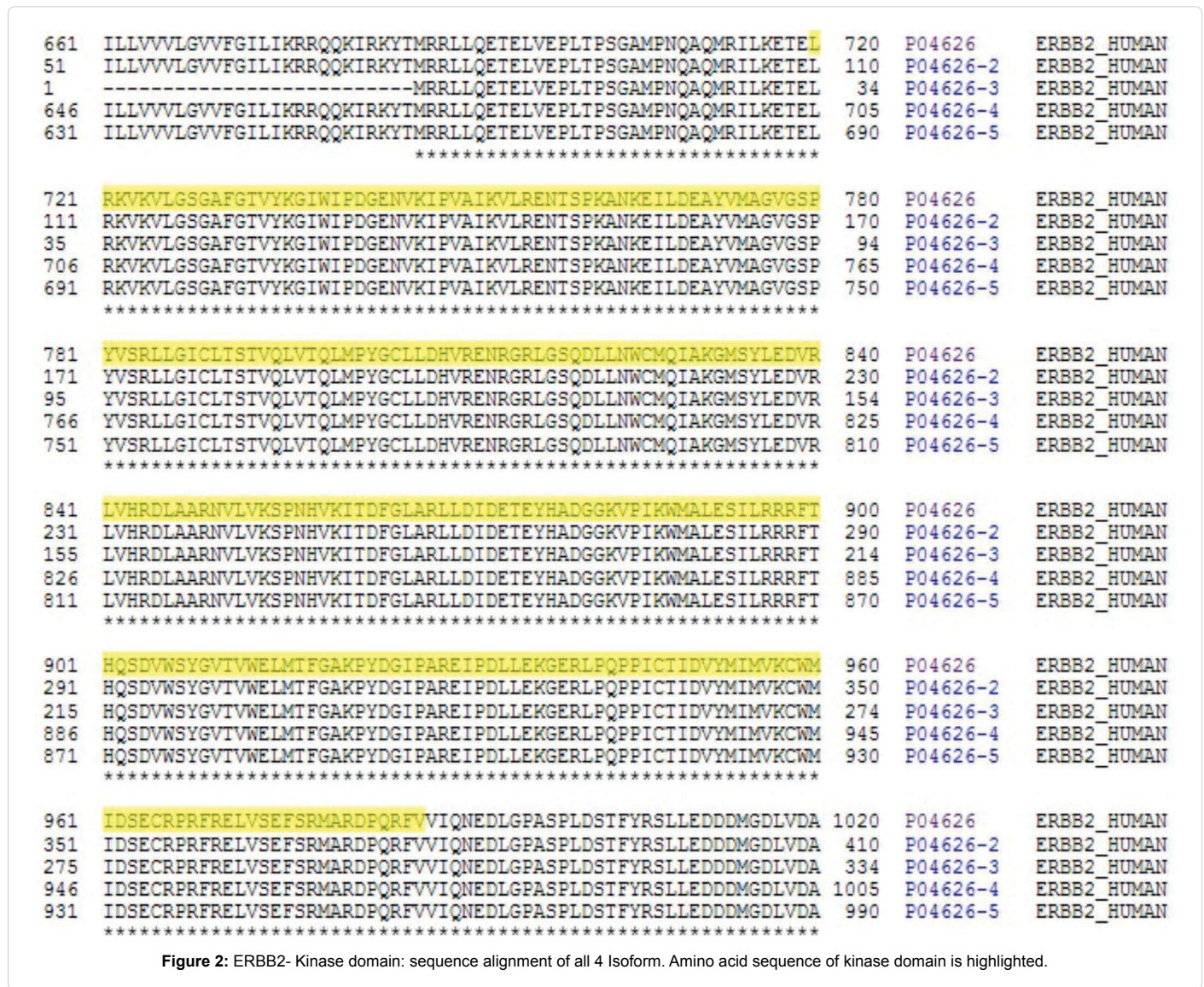
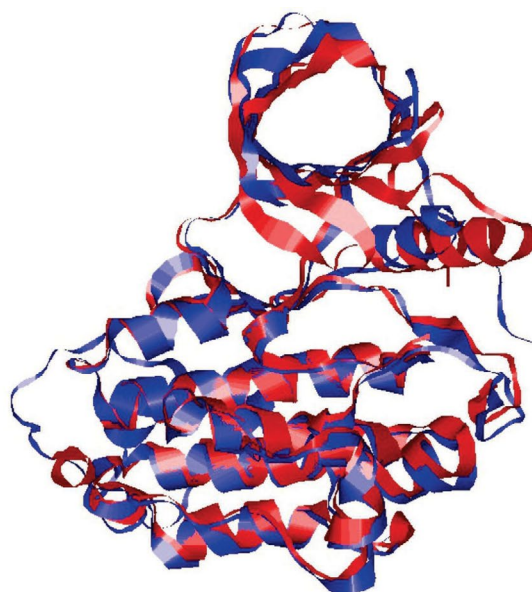


Figure 2: ERBB2- Kinase domain: sequence alignment of all 4 Isoform. Amino acid sequence of kinase domain is highlighted.



EQR:256Len1:307Len2:286score: 983.17Z-score:7.44RMSD:1.68SeqID:73%SeqSim:83%Cov1:87%Cov2:93%

4G5J:A	702:A	ALLRI LKETEFKKI KVLGS- - - - TVYKGLWI PEGEKVKI PVAI KE- - - - - KEI LDEAYVMASV- - - DN	771:A
3PP0:A	710:A	ALLRI LKETELRKVKVLGSGAF GTVYKGI WI PDGENVKI PVAI KVL RENTSPKANKEI LDEAYVMA G V GS	779:A
772:A		PHVCRL LGI CLTSTVQLI TQLMPFGCLLDYVREHKDNI GSQYLLNWCVQI AKGMNYLED RRLVHRDLAAR	841:A
780:A		PYVSRL LGI CLTSTVQLVTQLMPYGCLLDHVREN RGR LGSQDLLNWCMI AKGMSYLE DVRLVHRDLAAR	849:A
842:A		NVLVKTPQHVKI TDFGLAKLLGAE EKEYHAEGGKVPI KWMALES I LHRI YTHQSDVWSYGVT V WELMTFG	911:A
850:A		NVLVKSPNHVKI TDFGLARLLDI DETEYHA- - GKVPI KWMALES I LRRRFTHQSDVWSYGVT V WELMTFG	919:A
912:A		SKPYDGI PASEI SSI LEKGERLPQ PPI CTI DVYMI MVKCWMI DADSRPKFRELI I EFSKMARDPQR YLVI	981:A
920:A		AKPYDGI PAREI PDLLEKGERLPQ PPI CTI DVYMI MVKCWMI DSECRPRFRELVSEFSRMARDPQR FVVI	989:A
982:A		QG	983:A
990:A		QN	991:A

Figure 3: Three dimensional structure alignments of ErbB1 (PDB ID: 4G5J) and ErbB2 (PDB ID: 3PP0).

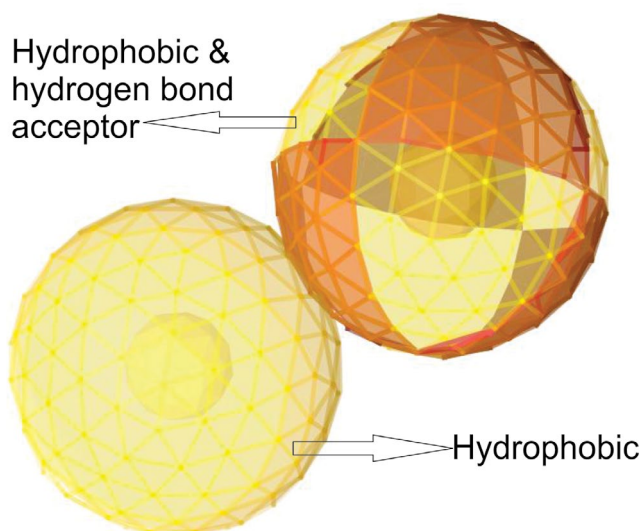


Figure 4: Shared Pharmacophore feature of the reference drugs Afatinib (DrugBank ID: DB08916) and Lapatinib (DrugBank ID: DB01259).

product molecules only 1,015 screened out were more poised. The significant reduction in the number of molecules could be attributed to the many stringent descriptors considered for this prediction. The descriptors considered were number of rotatable bonds, molecular weight, computed dipole moment, total solvent accessible surface area, total solvent-accessible volume, number of hydrogen bond donor, number of hydrogen bond acceptor, number of likely metabolic reactions, Van der Waals surface area of polar nitrogen and oxygen atoms and carbonyl carbon atoms, predicted central nervous system activity, hexadecane/gas partition coefficient, octanol/gas partition coefficient, water/gas partition coefficient, octanol/water partition coefficient, aqueous solubility, IC50 value for blockage of HERG K⁺ channels, apparent Caco-2 cell permeability in nm/sec, apparent MDCK cell permeability in nm/sec, brain/blood partition coefficient, binding to human serum albumin human oral absorption on 0 to 100% scale, and conformation-independent predicted aqueous solubility.

3D pharmacophore modelling and virtual screening

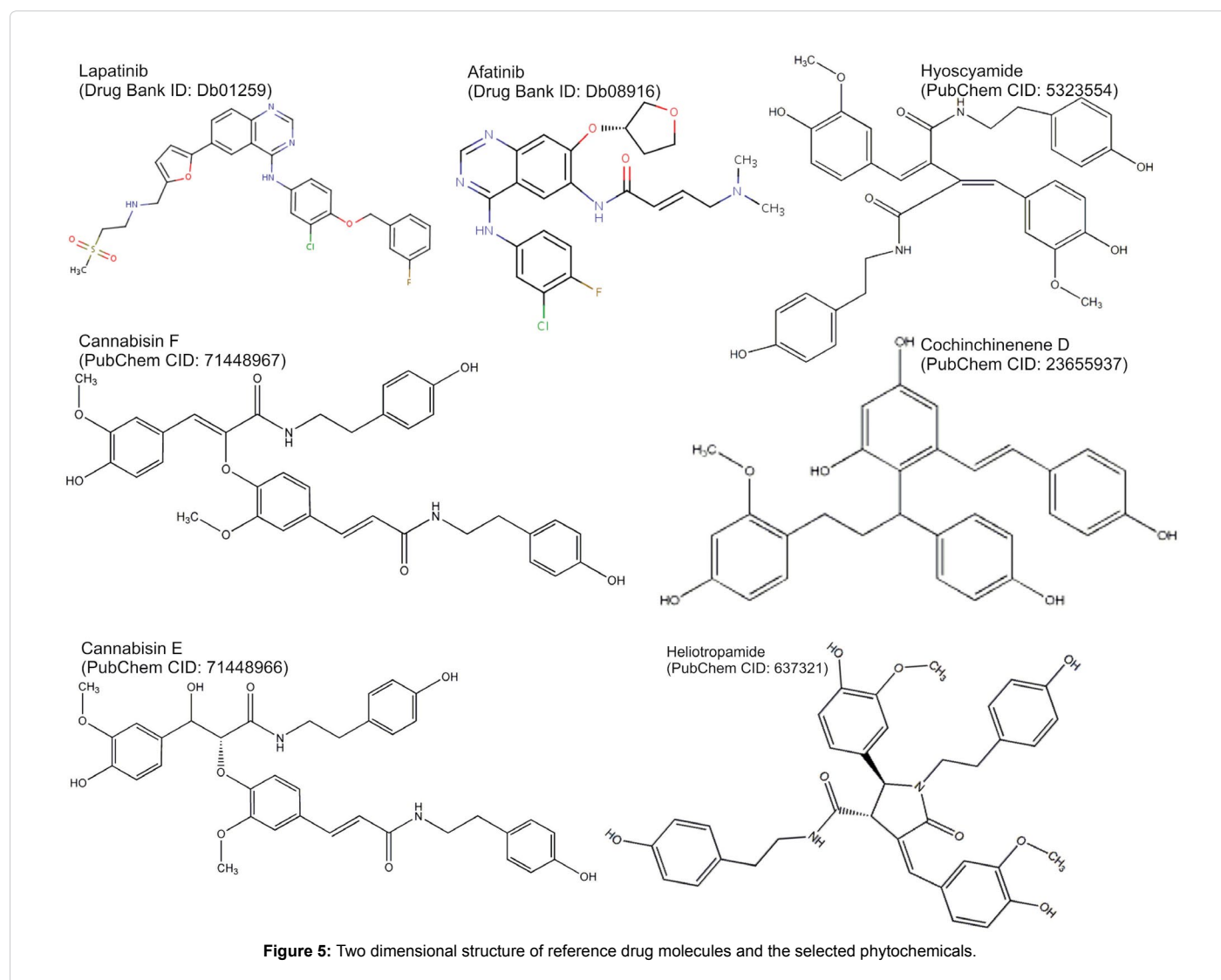
The structurally optimized drug molecules Afatinib and Lapatinib were aligned based on their pharmacophore features using LigandScout. Three shared features-two hydrophobic and one

hydrogen bond acceptor-were obtained from both the drugs (Figure 4), which were considered as a query for virtual screening. The 3D pharmacophore virtual screening demonstrated that among the 1,015 ADME passed natural product molecules, only 201 molecules have the pharmacophore features of both the drugs, and from the 1527 approved drugs, 356 molecules were matched with the query features. The ensued molecules were further confirmed by docking study.

Molecular docking and toxicity prediction

Molecular docking has played a key role in the identification of efficient binding of receptors and ligands. Compounds identified from docking studies with most favourable binding energy were considered as hits. The docking studies demonstrated that only 109 of the 201 natural product molecules and 125 of the 356 approved drugs have efficient binding with both the targets. Furthermore, only eighteen natural product molecules and five approved drugs were found to have a better docking score than the reference drug molecules.

Toxicity prediction had further elicited that out of the eighteen natural product molecules, only five molecules were non-toxic, which are all of plant origin.



The two-dimensional structure of the reference drug molecules, five best nontoxic natural product molecules and top five FDA approved drug molecules are shown in Figures 5 and 6. The MVD docking score is shown in Table 1. The selected phytochemicals had a docking score ranging from -144.25 Kcal/mol to -206.72 Kcal/mol and the top ranked approved drugs had a docking score ranging from -139.98 Kcal/mol to -201.28 Kcal/mol, which is better than that of the reference drug molecules. The docking result with hydrogen bond interactions are shown in Figures 7 and 8. Docking results of top five FDA approved drugs with ErbB1 and ErbB2 are shown in Figure 9. For better visualization, the hydrogen atoms of the proteins have been hidden. The number of hydrogen bonds and the interacting residues are shown in Tables 2 and 3. The reference drug molecules had one to four hydrogen bond interactions with the target. More importantly, the finalized phytochemicals and FDA approved drugs had six to twelve and one to eight hydrogen bond interactions, respectively. The docking score and number of hydrogen bonds of natural products and FDA approved drugs demonstrated the higher affinity with proteins than the reference drug molecules. Furthermore, a detailed analysis of the docking results showed that all ligands bonded with the kinase domains of the target.

Hyoscyamine is a nonalkaloidal component that is present in the seeds of *Hyoscyamus niger* [21]. Cannabidiol and Cannabichromene are acyclic bis-phenylpropane lignanamides existing in the fruits of *Cannabis sativa* [22]. It has been reported that another derivative of Cannabidiol possesses considerable anticancer property by arresting the S phase of the cell cycle [23]. *Cannabis sativa* is cultivated for seed oil, food, and medicine. Historically, tinctures, tea, and ointments have also been common preparations. In traditional Indian medicine, *C. sativa* has been used as a hallucinogenic, hypnotic, sedative, an analgesic, and anti-inflammatory agent [24]. Recently, a group of scientists from China

synthesized cannabidiol from vanillin [25]. Cannabidiol has already been reported for its cytotoxic activity [26], and cell-growth inhibitory activities against human lung cancer and human cervical cancer [27]. Cochinchinenone D from *Dracaena cochinchinensis* has already been reported for its antibacterial activities against *Helicobacter pylori* [28]. *Dracaena cochinchinensis* is predominant in China and its various other secondary metabolites are used to cure a variety of diseases, including neurodegenerative diseases, diabetes, and cancer [29,30]. Heliotropamide from *Heliotropium ovalifolium* has oxopyrrolidine-3-carboxamide central moiety [31]. A group of researchers from the United States of America synthesized Heliotropamide [32]. Although all five molecules are of plant source, they are not present worldwide and isolation of compounds is a very tedious procedure. Thus, it is paramount to perform their synthesis in a laboratory.

Fesoterodine, which is an approved drug, is a prodrug. It is broken down in-vivo into its active metabolite, 5-hydroxymethyl tolterodine (5-HMT), by plasma esterases. 5-hydroxymethyl metabolite exhibits an antimuscarinic activity. Both urinary bladder contraction and salivation are mediated via cholinergic muscarinic receptors. Therefore, acting as a competitive muscarinic receptor antagonist, fesoterodine ultimately acts to decrease the detrusor pressure owing to its muscarinic antagonism, thereby decreasing bladder contraction, and consequently, the urge to urinate [33-36]. Antrafenine is a piperazine derivative drug that acts as an analgesic and anti-inflammatory with an efficacy similar to that of naproxen. It is not widely used as it has largely been replaced by newer drugs [37,38]. Fluspirilene is a relatively long-acting injectable depot antipsychotic drug used for schizophrenia. It does not differ greatly from other depot antipsychotics (fluphenazine decanoate, fluphenazine enanthate, perphenazine onanthat, pipotiazine

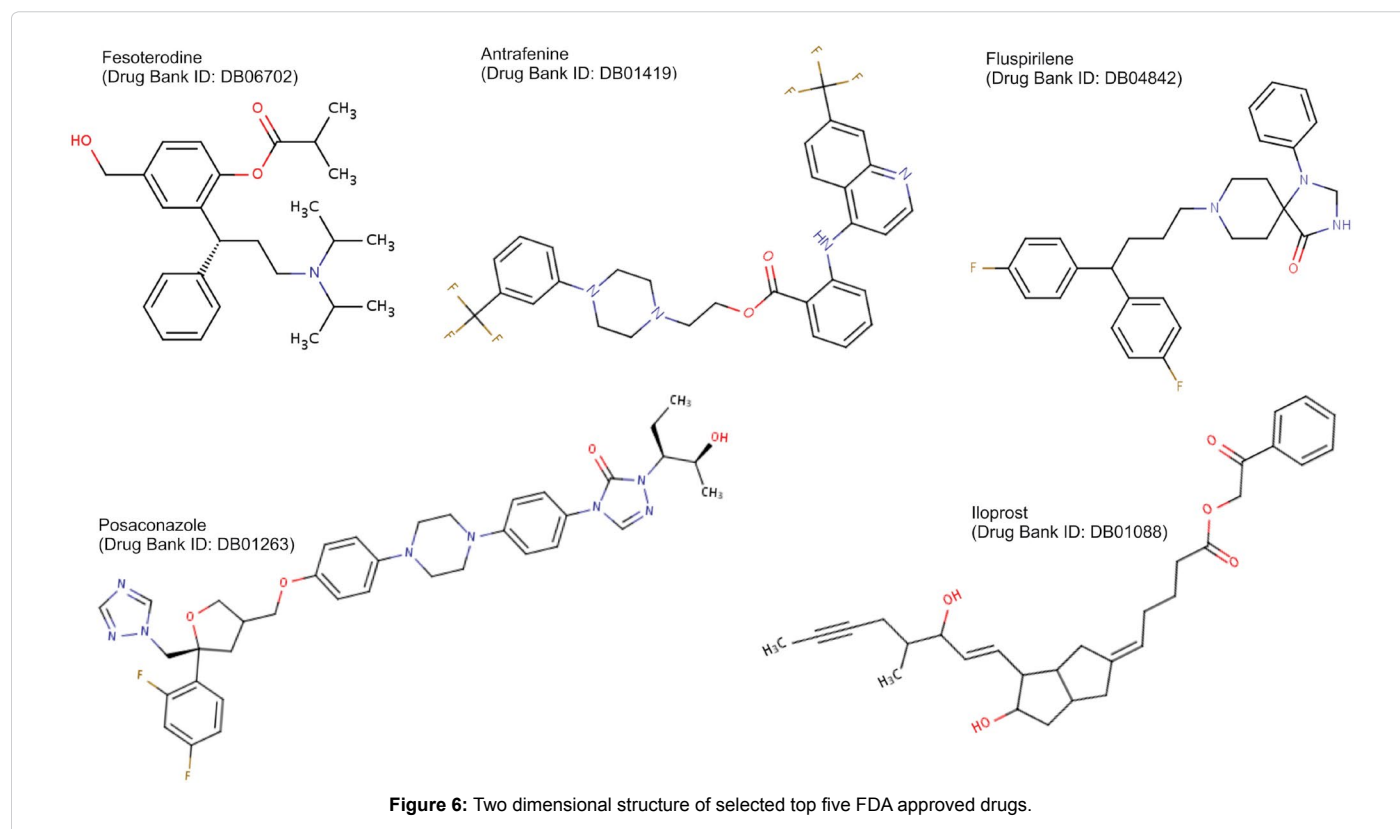


Figure 6: Two dimensional structure of selected top five FDA approved drugs.

Name	DrugBank ID / PubChem CID	ErbB1			ErbB2		
		MolDock Score (Kcal/mol)	Rerank Score	HBond	MolDock Score (Kcal/mol)	Rerank Score	HBond
Reference Drug							
Lapatinib	DB01259	-143.61	-111.05	-0.46	-180.07	-154.09	0.34
Afatinib	DB08916	-135.62	-94.54	-1.08	-171.46	-145.83	-4.73
Phytochemicals							
Hyoscyamide	CID 5323554	-169.50	-107.91	-12.96	-206.72	-151.38	-12.67
Cannabisin F	CID 71448967	-152.04	-102.19	-3.22	-203.89	-129.93	-5.98
Cochinchinenene D	CID 23655937	-153.32	-12.82	-18.04	-192.07	-145.30	-11.08
Cannabisin E	CID 71448966	-144.25	-80.66	-12.30	-184.77	-134.13	-0.58
Heliotropamide	CID 637321	-166.11	-103.16	-4.53	-180.75	-89.20	-6.94
FDA Approved drugs							
Fesoterodine	DB06702	-283.38	-67.59	-3.09	-201.28	-103.16	-9.52
Antrafenine	DB01419	-155.33	-106.60	-0.86	-201.03	-164.84	-1.07
Fluspirilene	DB04842	-139.98	-86.12	-0.36	-190.66	-153.02	-5.89
Posaconazole	DB01263	-141.70	-91.79	-4.41	-190.55	-120.98	-6.10
Iloprost	DB01088	-147.13	-48.72	-5.00	-189.66	-150.88	-2.35

Table 1: Docking score of reference drug molecules, phytochemicals, and top five FDA approved drugs with ErbB1 and ErbB2.

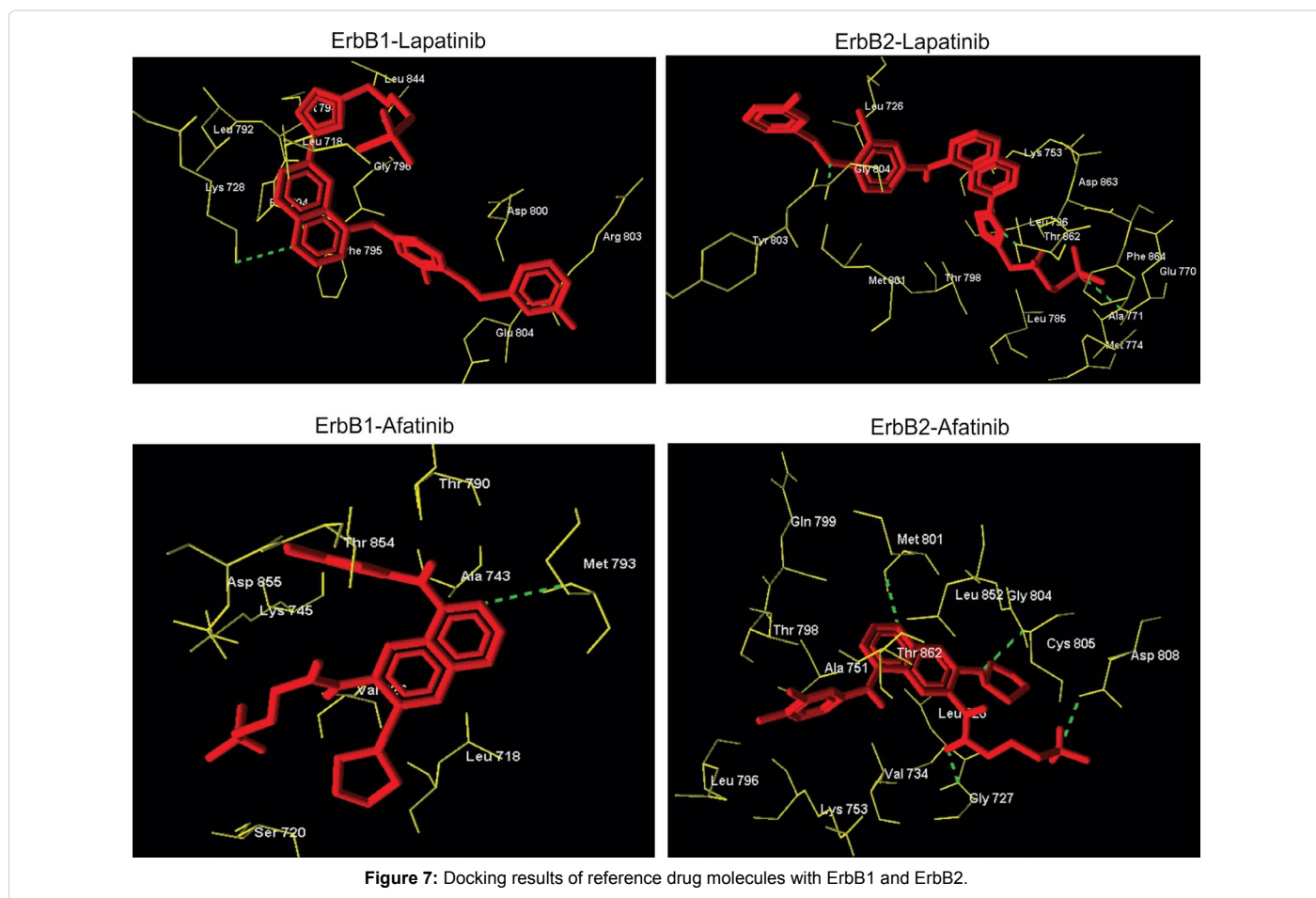


Figure 7: Docking results of reference drug molecules with ErbB1 and ErbB2.

undecylenate) with respect to treatment efficacy, response, or tolerability [39]. Posaconazole exerts its antifungal activity through blockage of the cytochrome P-450 dependent enzyme, sterol 14 α -demethylase, in fungi by binding to the heme cofactor located on the enzyme. This leads to the inhibition of the synthesis of ergosterol, a key component of the fungal cell membrane, and accumulation of methylated sterol precursors, which in turn

results in the inhibition of fungal cell growth, and ultimately, cell death [40,41]. Iloprost is a second generation structural analog of prostacyclin (PGI) with about tenfold greater potency than the first generation stable analogs, such as carbaprostacyclin. It binds with equal affinity to human prostacyclin (Prostanoid IP) and prostaglandin EP1 receptors, and constricts the ilium and fundus circular smooth muscle as strongly as prostaglandin E2 (PGE2)

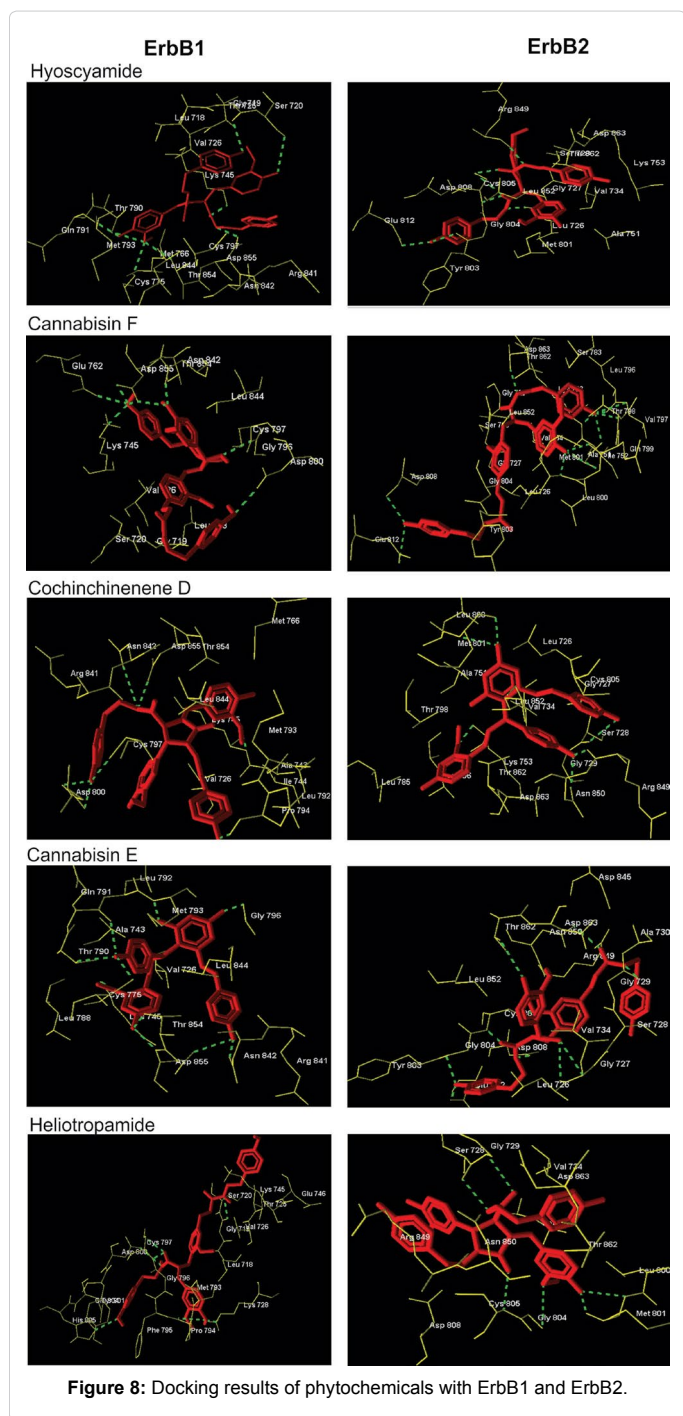


Figure 8: Docking results of phytochemicals with ErbB1 and ErbB2.

itself. Iloprost inhibits the ADP, thrombin, and collagen-induced aggregation of human platelets. In whole animals, iloprost acts as a vasodilator, hypotensive, and antidiuretic, and prolongs bleeding time. All of these properties help to antagonize the pathological changes that take place in the small pulmonary arteries of patients with pulmonary hypertension [42-46].

Conclusion

Afatinib and Lapatinib are the leading choice of drugs used for lung cancer. Both have a different inhibitory capacity to the highly expressed proteins ErbB1 and ErbB2 and also have many adverse reactions [46].

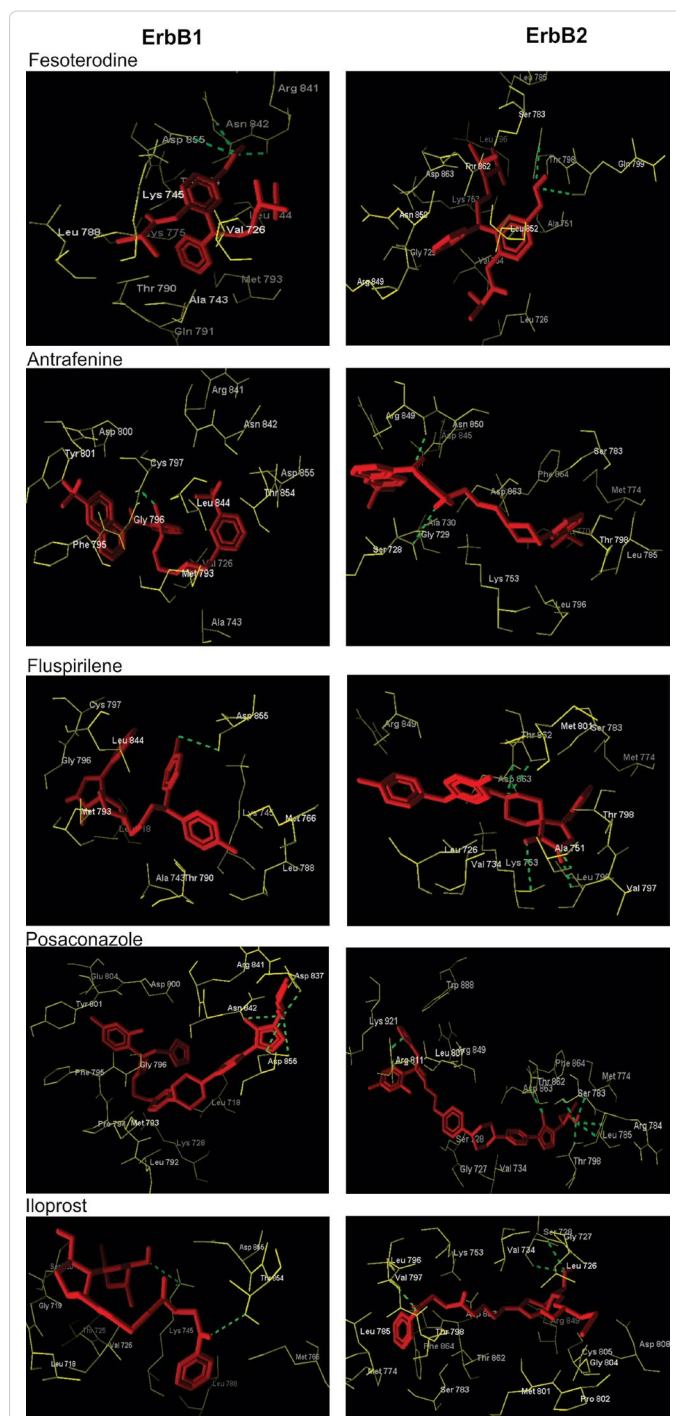


Figure 9: Docking results of top five FDA approved drugs with ErbB1 and ErbB2.

Although several previous studies have attempted at finding the best inhibitors, they have thus far failed to determine a common inhibitor targeting both the proteins. The current study achieved this by following an *in silico* approach. Five nontoxic phytochemicals Hyoscyamide, Cannabin F, Cochininenene D, Cannabin E, and Heliotropamide and five FDA approved drug molecules Fesoterodine, Antrafenine, Fluspirilene, Posaconazole, and Iloprost are capable of inhibiting both ErbB1 and ErbB2. The results obtained need to be confirmed biologically by conducting *in vivo* experiments.

Name	ErbB1		ErbB2	
	Number of Hydrogen Bonds	Interacting residues	Number of Hydrogen Bonds	Interacting residues
Lapatinib	1	Lys 728	3	Ala 771, Gly 804, Thr 862
Afatinib	1	Met 793	4	Gly 727, Met 801, Cys 805, Asp 808
Hyoscyamide	9	Gly 719, Ser 720, Lys 745, Cys 775, Thr 790 (2 hbonds), Gln 791, Thr 854, Asp 855	7	Leu 726, Gly 804, Cys 805 (3 hbonds), Glu 812, Arg 849
Cannabisin F	8	Lys 745, Glu 762, Cys 797, Asp 800, Asn 842, ASP 855 (3 hbonds)	12	Gly 729, Ala 751, Lys 753, Leu 796, Val 797, Thr 798, Gln 799, Leu 800, Met 801, Asp 808, Glu 812, Asp 863
Cochinchinenene D	10	Lys 745, Cys 775, Thr790, Gln 791, Met 793, Gly 796, Asn 842, Thr 854, Asp 855,(2 hbonds)	6	Ser 728, Lys 753, Met 801 (2 hbonds), Arg 849, Asn 850
Cannabisin E	7	Gly 719, Lys 728, Pro 794, Cys 797 (2 hbonds), Asp 800, His 805	11	Leu 726, Gly 727, Gly 729, Tyr 803, Cys 805 (2 hbonds), Asp 808, Glu 812, Arg 849, Asn 850, Thr 862
Heliotropamide	7	Lys 745, Pro 794, Cys 797, Asp 800 (2 hbonds), Asn 842, Asp 855	6	Ser 728, Gly 729, Met 801 (2 hbonds), Gly 804, Cys 805

Table 2: Number of Hydrogen Bonds and Interacting residues from the docking result of reference drug molecules and phytochemicals.

Name	ErbB1		ErbB2	
	Number of Hydrogen Bonds	Interacting residues	Number of Hydrogen Bonds	Interacting residues
Fesoterodine	3	Arg 841, Asn 842, Asp 855	2	Thr 798, Gln 799
Antrafenine	1	Cys 797	2	Gly 729, Arg 849
Fluspirilene	1	Asp 855	5	Ala 751, Lys 753, Leu 796, Thr 862, Asp 863
Posaconazole	4	Asp 837, Asn 842, Asp 855 (2 hbonds)	8	Ser 783 (2 hbonds), Arg 784, Leu 785, Thr 798, Arg 811, Thr 862, Asp 863
Iloprost	2	Lys 745, Thr 854	4	Ser 728 (2 hbonds), Val 797, Thr 798

Table 3: Number of Hydrogen Bonds and Interacting residues from the docking result of top five FDA approved drugs.

References

- www.who.int/mediacentre/factsheets/fs297/en/.
- Sharma SV, Bell DW, Settleman J, Haber DA (2007) Epidermal growth factor receptor mutations in lung cancer. *Nat Rev Cancer* 7: 169-181.
- www.cancerresearchuk.org/cancer-info/cancerstats/world/incidence/.
- Hynes NE, Lane HA (2005) ERBB receptors and cancer: the complexity of targeted inhibitors. *Nat Rev Cancer* 5: 341-354.
- Robinson DR, Wu YM, Lin SF (2000) The protein tyrosine kinase family of the human genome. *Oncogene* 19: 5548-5557.
- Tebbutt N, Pedersen MW, Johns TG (2013) Targeting the ERBB family in cancer: couples therapy. *Nat Rev Cancer* 13: 663-673.
- Singla S, Pippin JA, Drebin JA (2012) Dual ErbB1 and ErbB2 receptor tyrosine kinase inhibition exerts synergistic effect with conventional chemotherapy in pancreatic cancer. *Oncol Rep* 28: 2211-2216.
- George JJ, Umrana VV (2012) Subtractive genomics approach to identify putative drug targets and identification of drug-like molecules for beta subunit of DNA polymerase III in *Streptococcus* species. *Appl Biochem Biotechnol* 167: 1377-1395.
- Maramotti S, Paci M, Micciché F, Ciarrocchi A, Cavazza A, et al. (2012) Soluble epidermal growth factor receptor isoforms in non-small cell lung cancer tissue and in blood. *Lung Cancer* 76: 332-338.
- Shindyalov IN, Bourne PE (1998) Protein structure alignment by incremental combinatorial extension (CE) of the optimal path. *Protein Eng* 11: 739-747.
- Mayer AM, Gustafson KR (2008) Marine pharmacology in 2005-2006: antitumour and cytotoxic compounds. *Eur J Cancer* 44: 2357-2387.
- Mayer AM, Gustafson KR (2006) Marine pharmacology in 2003-2004: anti-tumour and cytotoxic compounds. *Eur J Cancer* 42: 2241-2270.
- LigPrep (2005) Schrödinger, LLC, New York.
- Maestro (2009) Schrödinger, LLC, New York.
- QikProp (2009) Schrödinger, LLC, New York.
- Wermuth CG, Ganellin CR, Lindberg P, Mitscher LA (1998) Glossary of terms used in medicinal chemistry (IUPAC Recommendations 1998). *Pure Appl Chem* 70: 1129-1143.
- Wolber G, Langer T (2005) LigandScout: 3-D pharmacophores derived from protein-bound ligands and their use as virtual screening filters. *J Chem Inf Model* 45: 160-169.
- Wolber G, Dornhofer AA, Langer T (2006) Efficient overlay of small organic molecules using 3D pharmacophores. *J Comput Aided Mol Des* 20: 773-788.
- Thomsen R, Christensen MH (2006) MolDock: a new technique for high-accuracy molecular docking. *J Med Chem* 49: 3315-3321.
- Hardy B, Douglas N, Helma C, Rautenberg M, Jeliakova N, et al. (2010) Collaborative development of predictive toxicology applications. *J Cheminform* 2: 7.
- Ma CY, Liu WK, Che CT (2002) Lignanamide and nonalkaloidal components of *Hyoscyamus niger* seeds. *J Nat Prod* 65: 206-209.
- Sakakibara I, Ikeya Y, Hayashi K, Okada M, Maruno M (1995) Three acyclic bis-phenylpropane lignanamide from fruits of *Cannabis sativa*. *Phytochemistry* 38: 1003-1007.
- Chen T, Hao J, He J, Zhang J, Li Y, et al. (2013) Cannabisin B induces autophagic cell death by inhibiting the AKT/mTOR pathway and S phase cell cycle arrest in HepG2 cells. *Food Chem* 138: 1034-1041.
- Wang L, Waltenerger B, Pferschy-Wenzig EM, Blunder M, Liu X, et al. (2014) Natural product agonists of peroxisome proliferator-activated receptor gamma (PPARgamma): a review. *Biochem Pharmacol* 92: 73-89.
- Xia YM, Xia J, Chai C (2014) Total synthesis of cannabisin F. *Chemical Papers* 68: 384-391.
- Chen JJ, Huang SY, Duh CY, Chen IS, Wang TC, et al. (2006) A new cytotoxic amide from the stem wood of *Hibiscus tiliaceus*. *Planta Med* 72: 935-938.
- Li YZ, Tong AP, Huang J (2012) Two New Norlignans and a New Lignanamide from *Peperomia tetraphylla*. *Chem Biodivers* 9: 769-776.
- Zhu Y, Zhang P, Yu H, Li J, Wang MW, et al. (2007) Anti-*Helicobacter pylori* and thrombin inhibitory components from Chinese dragon's blood, *Dracaena cochinchinensis*. *J Nat Prod* 70: 1570-1577.
- Li N, Ma Z, Li M, Xing Y, Hou Y (2014) Natural potential therapeutic agents

- of neurodegenerative diseases from the traditional herbal medicine Chinese dragon's blood. J Ethnopharmacol 152: 508-521.
30. Fan JY, Yi T, Sze-To CM, Zhu L, Peng WL, et al. (2014) A systematic review of the botanical, phytochemical and pharmacological profile of *Dracaena cochinchinensis*, a plant source of the ethnomedicine "dragon's blood". Molecules 19: 10650-10669.
 31. Guntern A, Ioset JR, Queiroz EF, Sándor P, Foggin CM, et al. (2003) Heliotropamide, a novel oxopyrrolidine-3-carboxamide from *Heliotropium ovalifolium*. J Nat Prod 66: 1550-1553.
 32. Younai A, Chin GF, Shaw JT (2010) Diastereoselective synthesis of (\pm)-heliotropamide by a one-pot, four-component reaction. J Org Chem 75: 8333-8336.
 33. Malhotra B, Dickins M, Alvey C, Jumadilova Z, Li X, et al. (2011) Effects of the moderate CYP3A4 inhibitor, fluconazole, on the pharmacokinetics of fesoterodine in healthy subjects. Br J Clin Pharmacol 72: 263-269.
 34. Malhotra B, Gandelman K, Sachse R, Wood N, Michel MC (2009) The design and development of fesoterodine as a prodrug of 5-hydroxymethyl tolterodine (5-HMT), the active metabolite of tolterodine. Curr Med Chem 16: 4481-4489.
 35. Mansfield KJ, Chandran JJ, Vaux KJ, Millard RJ, Christopoulos A, et al. (2009) Comparison of receptor binding characteristics of commonly used muscarinic antagonists in human bladder detrusor and mucosa. J Pharmacol Exp Ther 328: 893-899.
 36. Nilvebrant L (2002) Tolterodine and its active 5-hydroxymethyl metabolite: pure muscarinic receptor antagonists. Pharmacol Toxicol 90: 260-267.
 37. James MJ, Cook-Johnson RJ, Cleland LG (2007) Selective COX-2 inhibitors, eicosanoid synthesis and clinical outcomes: a case study of system failure. Lipids 42: 779-785.
 38. Moallem SA, Imenshahidi M, Shahini N, Javan AR, Karimi M, et al. (2013) Synthesis, Anti-Inflammatory and Anti- Nociceptive Activities and Cytotoxic Effect of Novel Thiazolidin-4-ones Derivatives as Selective Cyclooxygenase (COX-2) Inhibitors. Iran J Basic Med Sci 16: 1238-1244.
 39. Schotte A, Janssen PF, Gommeren W, Luyten WH, Van Gompel P, et al. (1996) Risperidone compared with new and reference antipsychotic drugs: in vitro and in vivo receptor binding. Psychopharmacology (Berl) 12: 57-73.
 40. Li Y, Theuretzbacher U, Clancy CJ, Nguyen MH, Derendorf H (2010) Pharmacokinetic/pharmacodynamic profile of posaconazole. Clin Pharmacokinet 49: 379-396.
 41. Schiller DS, Fung HB (2007) Posaconazole: an extended-spectrum triazole antifungal agent. Clin Ther 29: 1862-1886.
 42. Ghofrani HA, Rose F, Schermuly RT, Olschewski H, Wiedemann R, et al. (2002) Amplification of the pulmonary vasodilatory response to inhaled iloprost by subthreshold phosphodiesterase types 3 and 4 inhibition in severe pulmonary hypertension. Crit Care Med 30: 2489-2492.
 43. Idzko M, Hammad H, van Nimwegen M, Kool M, Vos N, et al. (2007) Inhaled iloprost suppresses the cardinal features of asthma via inhibition of airway dendritic cell function. J Clin Invest 117: 464-472.
 44. Mubarak KK (2010) A review of prostaglandin analogs in the management of patients with pulmonary arterial hypertension. Respir Med 104: 9-21.
 45. Nicolini FA, Mehta JL, Nichols WW, Saldeen TG, Grant M (1990) Prostacyclin analogue iloprost decreases thrombolytic potential of tissue-type plasminogen activator in canine coronary thrombosis. Circulation 8: 1115-1122.
 46. www.fda.gov/Drugs/InformationOnDrugs/ApprovedDrugs/default.htm.